

Studies on Tribological Characteristics of Centrifugally Cast SiC_p-Reinforced Functionally Graded A319 Aluminium Matrix Composites

E. Jayakumar^{1,3} · A. P. Praveen² · T. P. D. Rajan³ · B. C. Pai³

Received: 15 July 2018 / Accepted: 12 September 2018 / Published online: 3 October 2018
© The Indian Institute of Metals - IIM 2018

Abstract The concept of functionally graded materials is effectively applied to design and fabricate engineering components with location-specific wear resistance suited to the particular application. The present study describes the wear behaviour of centrifugally cast A319 aluminium functionally graded metal matrix composites (FGMMC) formed from 20 wt% SiC_p-reinforced composite. Liquid stir casting method is used for homogeneous metal matrix composite preparation followed by vertical centrifugal casting for FGMMC rings production. Microstructure analysis of specimen reveals a homogeneous distribution of SiC_p reinforcements for the gravity and a gradient particle distribution, in the radial direction forming different zones, for the centrifugal castings. The dry sliding wear behaviour is studied on a DUCOM pin-on-disc tribometer with steel disc and by using FGMMC pins produced from different zones. Wear studies show gradient tribological properties, within a component, with a maximum wear resistance at the particle rich region, lesser in transition zone and the minimum wear resistance at the inner zones. SEM observation confirms abrasive wear predominance by revealing the microgrooves and ploughing on the worn-out surfaces.

Keywords Centrifugal casting · FGM · Aluminium · Silicon carbide particle (SiC_p) · Abrasive wear

1 Introduction

The functionally graded materials (FGMs) are advanced composite materials having two or more phases with spatial variation in composition and/or microstructure [1]. FGM components can be tailored to achieve exterior superficial hardness with adequate interior toughness, which is hardly attainable by monolithic or homogeneous materials. FGMs can be processed by constructive methods like powder densification, lamination and coating techniques and by mass transport methods like electro-deposition, infiltration and centrifugal casting techniques. Among the various production methods, centrifugal casting is one of the simple pressure casting methods by which dense, fine grained structure, free of gas porosity FGM components can be produced easily and economically. In the centrifugal casting method, the melt (alloy/MMC) is poured into the rotating or spinning mould with the help of a pouring cup. Due to the induced centrifugal force, phases or particles will form different regions of concentrations in the castings. From the outer to the inner periphery, different radial zones formed on the ring are: a chill zone (near the outer periphery of a few millimetres thickness), the particles-rich zone, transition and the particle-depleted (/free) inner zones, respectively, in order. Within the casting, the positions of particle-rich zone and depleted zones are governed by densities of the matrix and the particles/phases. The extent of particle gradation and thickness of zones are mainly controlled by the magnitude of centrifugal acceleration, particle size, temperature, viscosity and cooling rate of melt [2]. In FGMs, the industrial

✉ E. Jayakumar
ejkumar@yahoo.com

T. P. D. Rajan
tpdrajan@rediffmail.com

¹ SCT College of Engineering, Thiruvananthapuram, Kerala 695018, India

² Vidya Academy of Science and Technology, Thrissur, Kerala 680501, India

³ CSIR-National Institute for Interdisciplinary Science and Technology, Thiruvananthapuram, Kerala 695019, India

Table 1 Chemical composition of A319 alloy

Details of alloy	Major alloying elements (%)		Minor alloying elements (%)						Al (%)
	Si	Cu	Mg	Fe	Mn	Zn	Ni	Ti	Al (balance)
A319 as per standards	5.5–6.5	3.0–4.0	0.10	1.00	0.50	1.00	0.35	0.25	86.3–91.5
A319 ingot used	6.35	3.87	0.072	0.205	0.34	0.148	0.046	0.14	88.83

interest is mainly focused on the opportunity of controlling the gradation of either the physical/chemical properties or both by microstructural manipulations for specialised applications.

Aluminium–silicon alloys have become the potential candidate materials for manufacturing automobile components such as pistons, clutch housings and cylinder liners. Their high strength to weight ratio and reasonably good wear resistance enables weight reduction of dynamic systems leading to a significant improvement in fuel economy [3, 4]. The aluminium matrix composites reinforced with ceramic particles exhibit higher wear resistance than aluminium alloys [5]. By a proper selection of the ceramic particle reinforcements and their selective spatial distribution, the wear resistance can be improved without altering the bulk toughness of the component [6]. The tribological properties are greatly affected by type, size and the volume fraction of reinforcements in addition to the influence of interfacial bonding between matrix and reinforcements [7]. Since steel is the most common material used in practice and aluminium is the successor, the steel–aluminium tribology–pair is generally used in the wear studies. Taking into consideration the superior properties of the aluminium matrix composites with respect to the weight to wear resistance ratio, this pair is also used as a reference pair [8]. In homogenous MMCs, the dry sliding wear studies are done for various sample geometries for a variety of metal matrices and reinforcement combinations with different volume fractions of reinforcements [9, 10]. The microstructure–property correlations and wear behaviour studies are also being conducted for different configurations of pin and disc materials, for different relative velocities and sliding distances, for a wide range of loads [11–17].

In the present study, the melt of MMC, of A319 aluminium alloy with 20 wt%, 23 μm sizes, SiC_p reinforcement particles, is prepared by liquid metal stir casting method and used in vertical centrifugal casting to produce FGMMC rings. Pins are prepared from different zones of FGMMC rings, and the dry sliding wear behaviour is studied with EN 31 steel disc on a DUCOM pin-on-disc tribometer. Brinell hardness (BHN) and microstructures in the radial direction of the castings along with SEM and stereo-micrographs of worn-out pin specimens are taken to

study the functional gradation due to the particle distributions. The main objective of the study is to evaluate the influence of SiC_p concentrations at different zones on the wear behaviour of FGMMC rings.

2 Materials and Methods

2.1 Materials

The hypoeutectic A319, Al–Si alloy, having moderate strength, good toughness, weldability, corrosion resistance and good casting qualities is used as the matrix alloy. The chemical composition analysis of the alloy used for MMC processing is carried out by SPECTRO MAXX optical emission spectrometer and is given in Table 1 along with standard composition. The SiC_p particles with average size of 23 μm and density of 3.2 g/cm^3 are used as reinforcements. They are cleaned initially by using distilled water; the final ultrasonic cleaning is done in an acetone bath, and they are dried before storing. The particles are preheated at 600 $^\circ\text{C}$ for 2 h before powder addition.

2.2 Processing

The FGMMC rings are produced in two steps: composite melt is processed by liquid stir casting and this melt is moulded into FGMMC ring in a vertical centrifugal casting machine. Liquid stir casting process is used to produce homogeneous metal matrix composites. The composite synthesis is carried out using a 10 kg clay graphite crucible in an electrical resistance heating furnace. A steady vortex is created and maintained in the A319 alloy melt by a mechanical stirrer connected to a hydro-drive motor which rotates nearly at 300 rpm. In a controlled feed rate, the preheated SiC_p particles are added to the vortex of the melt at 740 $^\circ\text{C}$. The melt degassing is carried out by nitrogen gas purging at 720 $^\circ\text{C}$ for 45 min. After a good hand stirring, a portion of the melt is poured into the preheated metal moulds to get gravity castings. Meanwhile, the preheated metal ring mould is fixed to the vertical shaft of a centrifugal casting machine and kept under rotation at a constant speed of 1300 rpm. By using a pouring cup, the melt, at 760 $^\circ\text{C}$, is poured into the rotating mould to

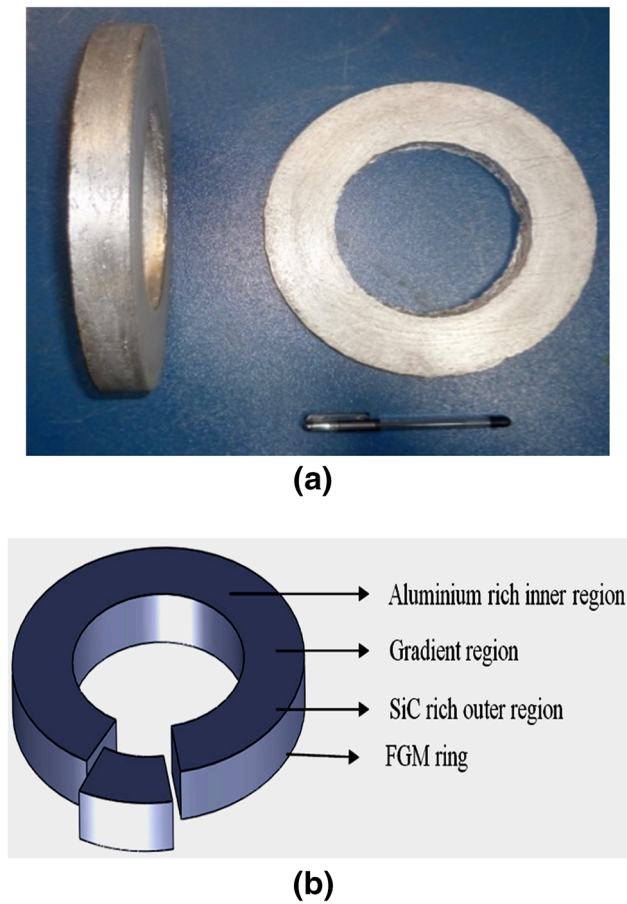


Fig. 1 aAs-cast FGMMC rings, b microstructure specimen and regions in the casting

produce the FGMMC rings. Figure 1a shows the centrifugally cast FGMMC rings, and Fig. 1b schematically represents the different zones observed in the ring.

2.3 Characterisation

From gravity and FGM castings, the required samples for mechanical, tribological and metallographic characterizations are prepared and heat treated. A319 alloy is a precipitation-hardening alloy. The standard heat treatment procedure (T6 condition) of solution heat treatment at 505 °C for 8 h subsequently quenched in warm water and then age hardened at 155 °C for 5 h is followed [18]. The optical microstructures are taken using DMRX Leica optical microscope. INDENTEC is used for conducting Brinell hardness tests for specimens in both as-cast and heat-treated conditions. A dry linear wear test is carried out in a DUCOM pin-on-disc tribometer with EN 31 steel disc and heat-treated FGM pins taken from different zones of the castings, and the dimensions of the pin are 6 mm diameter and 30 mm length. Each test is conducted with the following conditions: with a relative velocity of 2 m/s

for a sliding distance of 1800 m for 15-min duration. The tests are conducted at four different loading conditions (1, 2, 3 and 4 kg), and the wear rate behaviour of the FGM pins is calculated by weight loss method. For a better understanding of the involved wear mechanisms, the surface morphology of the worn-out pins is studied by Zeiss stereo-microscope and the SEM microstructures are taken by Jeol Scanning Electron Microscope.

3 Results and Discussion

3.1 Microstructural Characteristics

Figure 2a shows the optical micrographs of A319 aluminium alloy in the gravity cast condition. The various phases observed are dark needle-like eutectic silicon, the grey CuAl_2 and white $\alpha\text{-Al}$ matrix [19]. Evenly spaced secondary dendritic arms are also visible. The optical micrograph of A319-20SiC_pMMC gravity cast in as-cast condition, Fig. 2b, shows a uniform distribution of silicon carbide particles in the matrix. Figure 3 shows the optical micrographs of the centrifugally cast A319 alloy ring taken from similar locations as that from A319-20SiC_pFGMMC castings. No phase segregation or agglomerations are observed in any of the regions of the ring. From inner towards outer periphery in a radial direction, a gradual grain refinement is observed with lesser porosities.

Figure 4 shows the optical micrographs of the A319-20SiC_pFGMMC ring taken from the inner to the outer periphery in the radial direction at different zones; namely the innermost zone which is free of reinforcement particles, the transition zone, the particle-rich zone and the outer most chilled zone having a radial thickness of 2–3 mm. The density of the SiC_p is 3.2 g/cm³, and that of the aluminium alloy is 2.68 g/cm³. Due to the centrifugal effect, the higher density SiC_p particles move from the inner region towards the outer region in a radial direction. In Fig. 4a, the inner region of radial thickness 10–15 mm, shows a region in the casting free of reinforcement particles and having the fewer density impurities like slag inclusions and gas porosities. The centrifugal force and the solidification front will move the lighter gas bubbles and agglomerated particles, in the MMC melt, to diffuse and segregate towards the inner regions of the FGM castings. Before the actual testing or applications, in order to get dense porous free components, the inner regions can be removed by machining. In Fig. 4b, the transition region of 15–30 mm radial thickness, shows a gradual increase in reinforcements from free inner region towards the particle-rich region (Fig. 4c) (located nearer to the outer periphery) leading to a functionally graded microstructure. The region in the extreme outer periphery, the chilled zone (Fig. 4d), shows a less particle

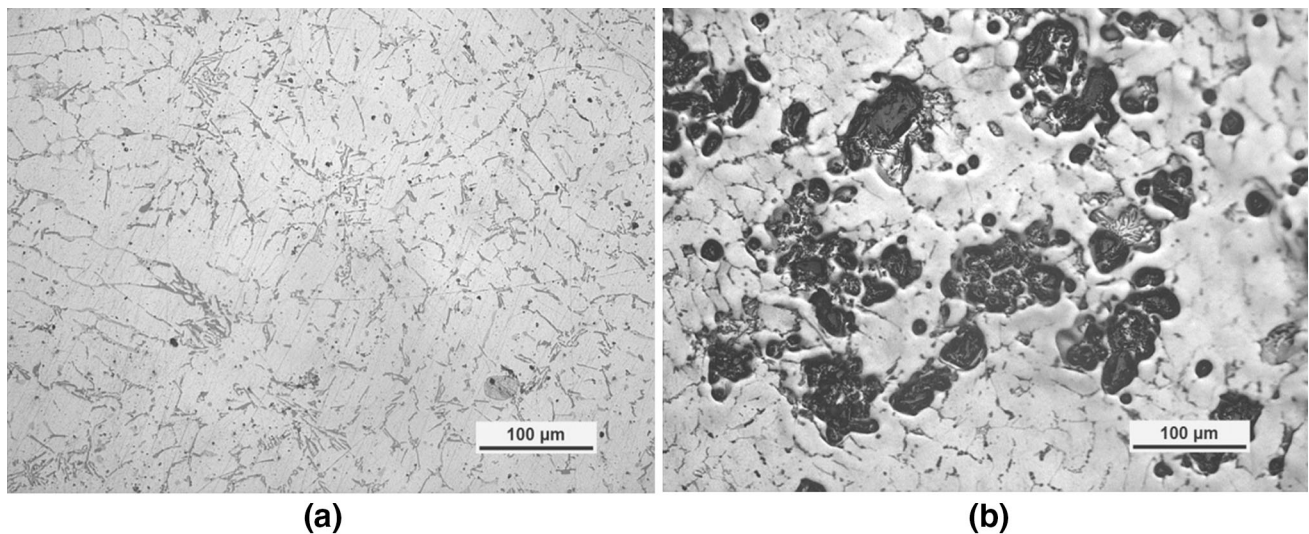


Fig. 2 Microstructure of gravity castings. **a** A319 alloy, **b** A319-20 SiC composite

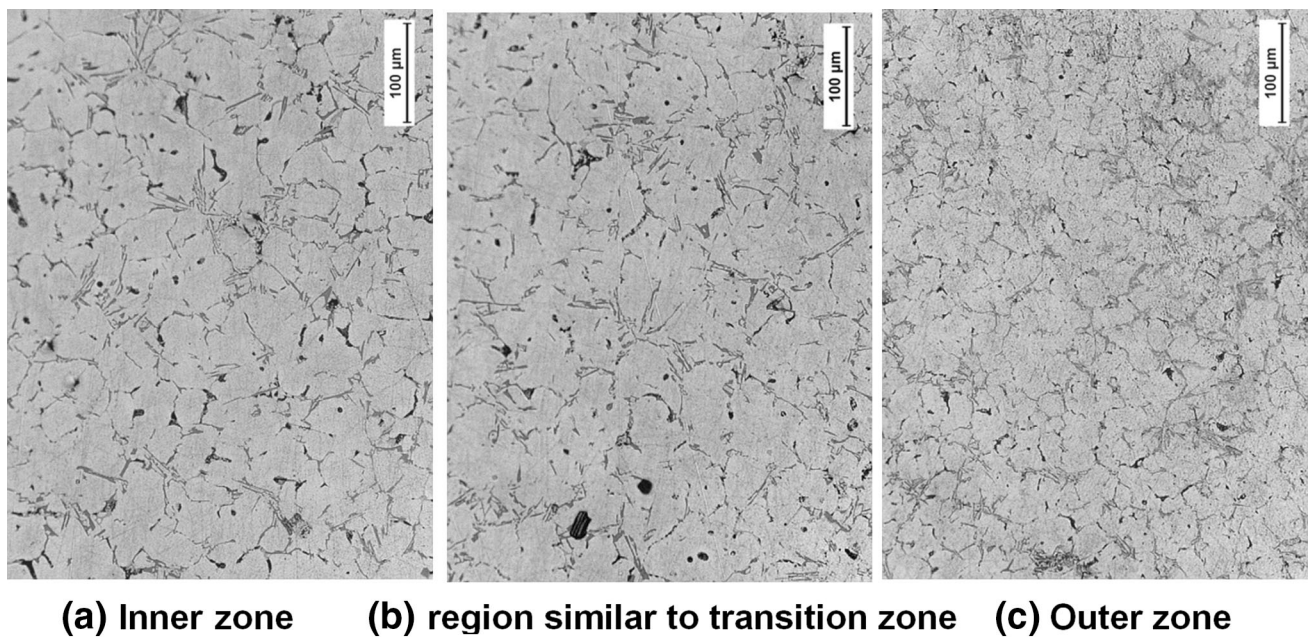


Fig. 3 Microstructures of A319 centrifugal casting from the inner to outer zone of the casting at similar locations as those of FGMMC castings. **a** Inner zone, **b** region similar to transition zone, **c** outer zone

concentration compared to the adjacent region due to the chill zone formation during pouring caused by the immediate solidification of the liquid composite melt which comes in contact with the surface of the rotating mould. The outer region closer to the chill zone will get a higher concentration of the particles due to the centrifugal force. The higher concentration of SiC_p towards the outer periphery strongly influences the hardness and wear resistance while the aluminium base alloy determines the properties in the particle-depleted inner zone which is comparatively lesser than that of the rich zone. Figure 5

shows the panoramic views of the microstructures of A319 FGM and A319-20 SiC_p FGMMC castings from inner diameter towards the outer diameter in the radial direction. Figure 5b clearly shows the microstructure variations in the different zones even at lower magnification. In case of A319 FGM, from Fig. 5a, the absence of multiphase in composition leads to minimum gradation and property changes. A well defined transition region is not observed in the microstructure, so for further studies of wear analysis for A319 FGM, only two zones (namely inner and outer zones) are considered.

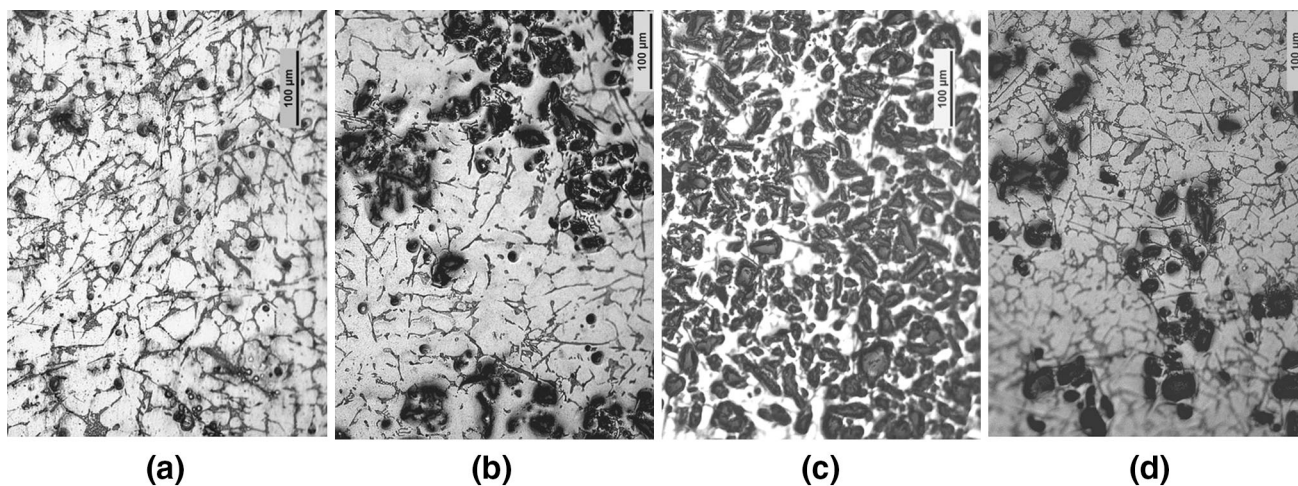
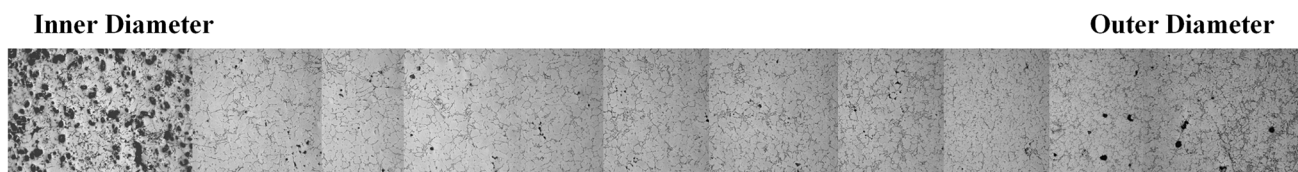
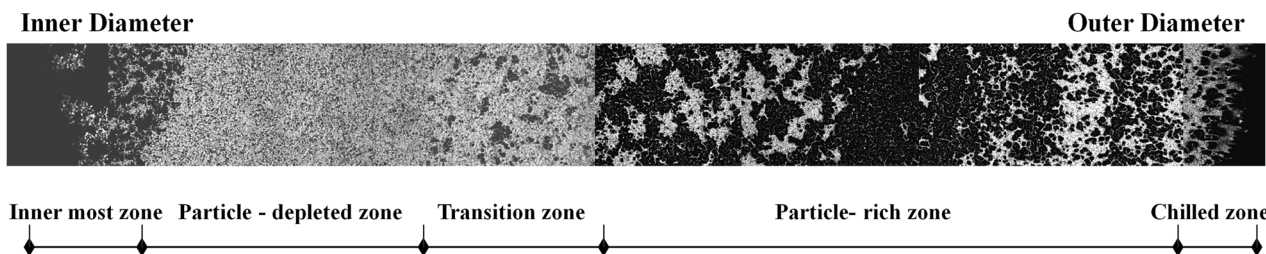


Fig. 4 Microstructures of A319-20SiC_pFGMMC from the inner to outer periphery of the casting. **a** Inner matrix rich zone/powder-depleted region (average zone size 15–20 mm radial thickness), **b** transition zone (average zone size 10–20 mm radial thickness), **c** particle-rich zone (average zone size 15–25 mm radial thickness), **d** outer most periphery/ chilled zone (average zone size 2–3 mm radial thickness)



(a) Panoramic view of microstructures of A319 FGM from inner to outer diameter in the radial direction



(b) Panoramic view of microstructures of A319-20 SiC_pFGMMC from inner to outer diameter in the radial direction

Fig. 5 Panoramic view of the microstructures of **a** A319 and **b** A319-20SiC_pFGMMC rings from the inner periphery of the ring towards the outer periphery along the radial direction

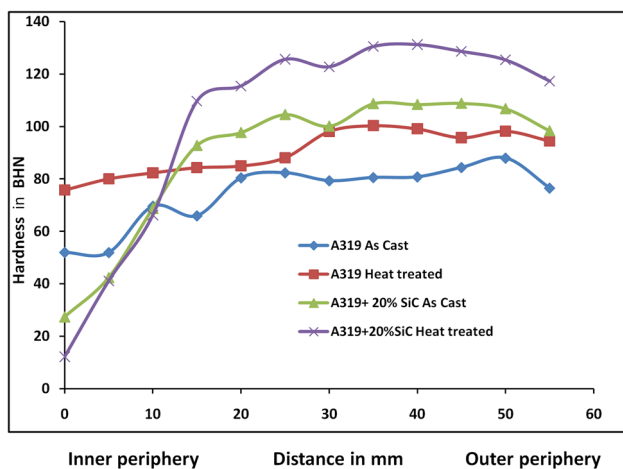
3.2 Hardness Behaviour

Table 2 shows the average Brinell hardness values of homogeneous gravity castings. The variations of average hardness in FGM rings, from inner periphery towards the outer periphery, of A319 alloy and A319-20SiC_pMMC in both as-cast and heat-treated conditions are shown in Fig. 6. Homogeneous gravity casting of A319 base alloy has a hardness of 84 BHN in the as-cast condition and is

raised to 95 BHN after the heat treatment. At the outer periphery of the A319 alloy centrifugal casting, the hardness value before and after the heat treatment are 76 BHN and 94 BHN, respectively. Since there is neither addition of SiC_p nor segregation of alloy phases, the variations in the hardness values are less from the middle region of the centrifugal casting towards the outer periphery in both conditions (as-cast and heat-treated). In the as-cast condition, the highest hardness value achieved

Table 2 Hardness of A319 and A319-20SiC homogeneous gravity die casting and centrifugal FGM castings under as-cast and T6 heat-treated conditions (in BHN)

Material	Gravity castings (BHN)		Centrifugal castings (BHN)	
	As-cast condition	Heat-treated condition	As-cast condition Particle-rich region	Heat-treated condition Particle-rich region
A319 alloy	84	95	87	100
A319-20SiC	91	110	108	131

**Fig. 6** Hardness variation of A319 alloy and A319-20SiC_pFGMMC rings in as-cast and T6 heat-treated conditions. (Shown from the inner periphery of the ring towards the outer periphery of the FGM ring measured along the radial direction). (FGMMC pins are prepared from the SiC particles-rich outer zone, transition zone and aluminium-rich inner zone of the ring. A319 alloy ring pins are prepared from only inner and outer zones. Test is conducted after T6 heat treatment)

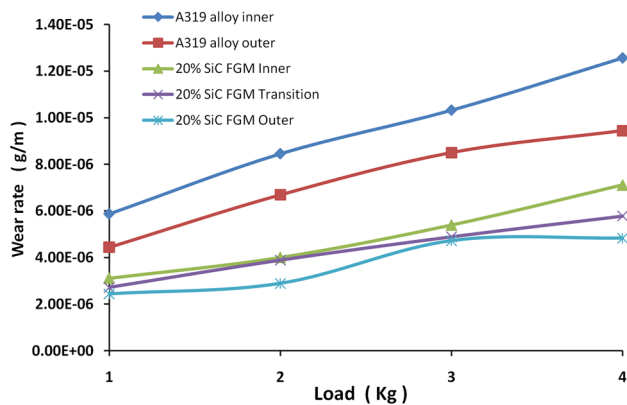
is 87 BHN at a distance of 20 mm from the outer periphery towards inner one and it increases to 100 BHN after heat treatment. The variation in hardness is mainly contributed by the grain refinement produced by the effects of centrifugal casting, which is similar to that of a pressure casting.

Homogeneous gravity casted A319-20SiC_pMMC has a hardness value of 91BHN in the as-cast condition and the hardness increases to 110 BHN after the heat treatment. At the outer periphery, the hardness value of FGMMC ring is 98 BHN in the as-cast and after heat-treated it increases to 117 BHN. A maximum hardness value of 108 BHN in as-cast and 131 BHN in heat-treated conditions are obtained. In the particle graded region, the hardness varies between 100 and 108 BHN in as-cast and is raised to 122–131 BHN in heat-treated conditions. The region near the innermost peripheries shows very low hardness due to the presence of gas porosities and agglomerated particles, which are segregated by the centrifugal force and the solidification front.

3.3 Wear Behaviour

The pin samples of 6 mm diameter and 30 mm length are prepared from gravity and centrifugal castings and are heat-treated at T6 conditions before the testing. Each test is conducted for a sliding distance of 1800 m with a relative velocity of 2 m/s, between the stationary pin and rotating steel disc, for 15-min test duration at four different loading conditions (1, 2, 3 and 4 kg). The wear rate behaviour of the FGM pins is calculated by weight loss method. Figure 7 shows the wear rate values of A319 alloy and A319-20SiC_pFGMMC pins prepared from different zones of the rings.

For A319 alloy centrifugal castings, since in the expected so-called transition region, the variations in microstructures as well as hardness values are minimal, only the inner zone and the outer region pins are prepared and the wear tests are conducted. A319 alloy inner pin shows a minimum wear rate of 5.8×10^{-6} g/m at a load of 1 kg and a maximum of 12.6×10^{-6} g/m at 4 kg. Similarly, the outer pin shows a minimum wear rate of 4.4×10^{-6} g/m at 1 kg and a maximum of 9.4×10^{-6} g/m at a load of 4 kg; these wear rate values are much lesser than those in the inner pins of the same ring. It is also

**Fig. 7** Wear rate versus load of A319 alloy and A319-20SiC_pFGMMC rings. Pins from **a** A319 alloy ring inner zone, **b** A319 alloy ring outer zone, **c** A319-20 SiC_p FGMMC ring inner zone, **d** A319-20 SiC_p FGMMC ring transition zone, **e** A319-20 SiC_p FGMMC ring outer zone

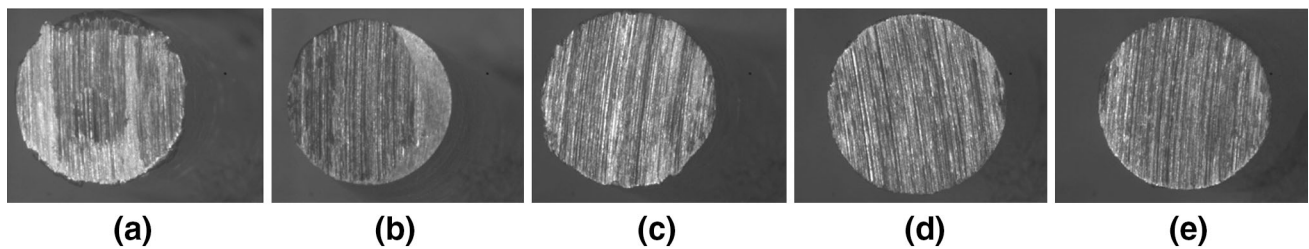


Fig. 8 Stereo-micrographs of pin (6 mm diameter) worn-out surfaces at 4 kg load (maximum loading condition)

evident that the outer zone of the A319 alloy ring shows a better wear resistance due to the refined grains, which leads to a higher hardness than the inner zones.

In case of A319-20SiC_pFGMMC castings, wear tests are conducted using pins prepared from three different regions, namely particle-depleted inner, transition and particle-rich outer zones. Inner pin shows a wear rate of 3.1×10^{-6} g/m at a load of 1 kg and 7.1×10^{-6} g/m at 4 kg, while the transition pin shows 2.7×10^{-6} g/m and 5.7×10^{-6} g/m and the outer pin shows a wear rate of 2.4×10^{-6} g/m and 4.8×10^{-6} g/m, respectively, at 1 kg and 4 kg loads. It is observed that the wear rate is steadily increasing with the increase in applied load. For all conditions, the wear rate of FGM outer specimen shows the minimum than that of other specimens in the similar conditions. The graphs indicate that the SiC particles on the aluminium matrix alloy decreases the wear rate due to their higher hardness and the strong bonding with aluminium matrix, thus protecting the surface against the severe destructive action of the abrasives. The strong interfacial bond plays a critical role in transferring the loads from the matrix to the reinforcements, resulting in less wear. At low-load conditions, the SiC particles protrude and protect the contact surface from material loss by reducing the real area of contact. The transition from mild to severe (metallic) wear is associated with the existence of a delamination wear process. Although reported that Si additions (4–24%Si) improves wear resistance of aluminium, no relationship between wear rates as a function of Si content is found. Wear rate increases linearly with applied pressure but is independent of sliding velocity. The value of the friction coefficient is found to be insensitive to the applied pressure, the percentage of Si content and the sliding velocity. In the wear analysis, the mutual transfer of material between the wearing Al–Si and the steel counterface appears to be a feature of all wear regimes and becomes more significant as load (pressure) increases and no transition in wear mechanism is observed with increased pressure [20].

3.4 Tribo-surface Morphology

From stereo-micrographs, at all loading conditions even at the maximum load of 4 kg, only the finer abrasion grooves are visible in the surface morphology of the worn-out surfaces of A319 alloy FGM and A319-20SiC_pFGMMC wear pins (Fig. 8). SEM micrographs of wear surfaces (Fig. 9) reveal the various surface characteristics of wear, namely abrasion grooves (A), cracks (B), craters (C), fine wear debris (D) and oxide layers (E), indicating that mild wear conditions are prominent. The oxidised surface characteristics and scoring on surfaces suggest that they are the major wear mechanisms responsible for material loss [21, 22]. Fine debris generated during dry sliding has two contradictory roles. They may get locked between the sliding surfaces and promote the three-body wear, which enhances the volume loss in wear. On the other hand, the hard oxide particles in the debris may be locked between the sliding surfaces and get compacted to form a protective tribolayer so that there are no scoring marks on the wear surfaces. Apart from adhesion, micro-cutting and abrasion, the tribolayers also flake off during dry sliding wear.

4 Conclusions

A319-20SiC_pFGMMC is produced successfully by a vertical centrifugal casting method. Microstructure analysis of FGMMC ring shows the gradient distribution of SiC_p reinforcements forming different zones in the casting and hardness distribution confirms it. Wear behaviour of A319-20SiC_pFGMMC largely depends upon the concentration of SiC_p particles. SiC_p-rich outer zones show lesser wear rate in comparison with other regions. The linear variation of wear rate with applied load is observed. Fine grooves and cracks are seen, and it is clear that the minor abrasion is the major-involved wear mechanism. Oxide layer formation is clearly visible, and this prevents the surface from major wear up to a certain transition load. The enhanced interface temperature at higher load weakens the interface bond between silicon particle and aluminium matrix leading to higher wear rate. Addition of SiC_p and heat treatment

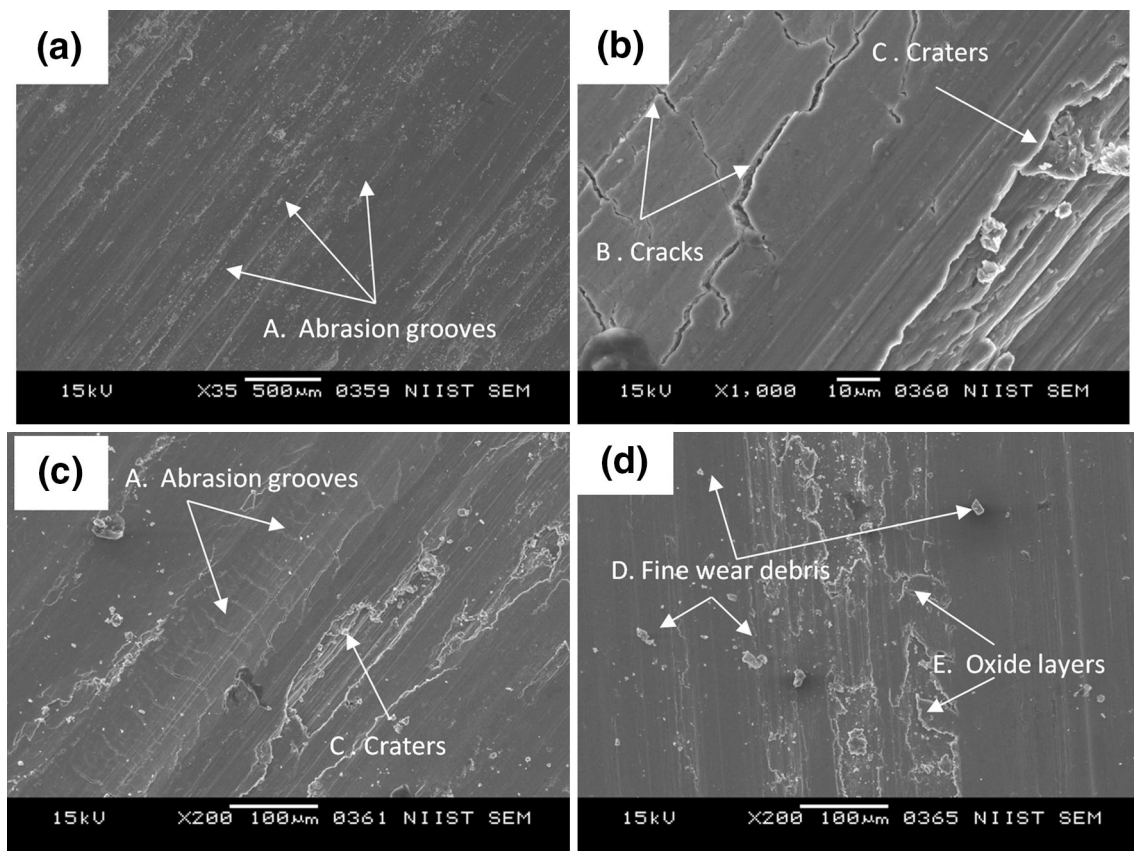


Fig. 9 SEM micrographs taken from various locations of a wear-tested outer pin of A319-20SiC_p FGMMC at 4 kg load (A, abrasion grooves; B, cracks; C, craters; D, fine wear debris; and E, oxide layers)

provide remarkable improvements in the wear resistance of the FGM compared to the alloy. The study clearly depicts the gradient nature in the structure and properties of the FGMMC rings that provide an improved wear resistance property near the outer periphery of the rings.

Acknowledgements The authors are grateful to the director, CSIR-NIIST, and members of Materials Science and Technology Division, CSIR-NIIST, for their support during the work.

References

- Rajan T P D, Pillai R M, and Pai B C, *Int J Cast Met Res*, **21** (2008) 1.
- Nairobi B D, Humberto Melgarejo Z, and Marcelo Sua´rez O, *Mat Char* **55** (2005) 167.
- Karamis M B, Alper Cerit A, Selcuk B, and Nair F, *Wear* **289** (2012) 73.
- Md Aminul Islam, and Zoheir N Farhat, *Tribol Int* **44** (2011) 498.
- Kennedy F E, Balbahadur A C, and Lashmore D S, *Wear* **203–204** (1997) 715.
- Vieira A C, Sequeira P D, Gomes J R, and Rocha L A, *Wear* **267** (2009) 585.
- Rosenberger M R, Schvezov C E, and Forlerer E, *Wear* **259** (2005) 590.
- Chen R, Iwabuchi A, and Shimizu T, *Wear*, **238** (2000) 110.
- Kumar D, Roy H, and Show B K, *Tribol Trans* **58** (2015) 518.
- Singh S, Garg M, and Batra N K, *Tribol Trans* **58** (2015) 758.
- Shorowordi K M, Haseeb A S M A, and Celis J P, *Wear* **256** (2004) 1176.
- Natarajan N, Vijayarangan S, and Rajendran I, *Wear* **261** (2006) 812.
- Majumdar J D, Chandra B R, and Manna I, *Wear* **262** (2007) 641.
- Das S, Mondal D P, Sawla S, and Ramakrishnan N, *Wear* **264** (2008) 47.
- Shivamurthya R C, and Surappa M K, *Wear* **271** (2011) 1946.
- Ozben T, Kilickap E, and Orhan C, *J Mater Process Technol* **198** (2008) 220.
- Goto H, and Omor S, *Tribol Trans* **43** (2000) 57.
- Tavitas-Medrano F J, Gruzleski J E, Samuel F H, Valtierra S, and Doty H W, *Mater Sci Eng A* **480** (2008) 356.
- Dwivedi D K, *Mater Des* **31** (2010) 2517.
- Deuis R L, Subramanian C, and Yellup J M, *Compos Sci Technol* **57** (1997) 415.
- Rajeev V R, Dwivedi D K, and Jain S C, *Mater Des* **31** (2010) 4951.
- Miracle D B, *Compos Sci Technol* **65** (2005) 2526.